

# Ambipolar field-effect transistor characteristics of (BEDT-TTF)(TCNQ) crystals and metal-like conduction induced by a gate electric field

Masatoshi Sakai,\* Hirotaka Sakuma, Yuya Ito, Akinobu Saito, Masakazu Nakamura, and Kazuhiro Kudo  
*Department of Electronics and Mechanical Engineering, Chiba University, 1-33 Yayoi-cho, Inage-ku, Chiba 263-8522, Japan*

(Received 3 April 2007; published 18 July 2007)

Ambipolar carrier conduction has been observed in a metal-insulator-semiconductor field-effect transistor made using (BEDT-TTF)(TCNQ) crystals. The temperature dependence of the source current with the applied positive gate voltage exhibits metal-like behavior at around room temperature. The metal-like conduction transforms into thermal-activation-type behavior below 240 K. The  $I_S$ - $V_{DS}$  curve for an applied gate voltage of 80 V exhibited a corresponding change in the curvature below 240 K.

DOI: [10.1103/PhysRevB.76.045111](https://doi.org/10.1103/PhysRevB.76.045111)

PACS number(s): 71.30.+h, 85.30.Tv, 73.40.Qv, 85.65.+h

## I. INTRODUCTION

The effect of the gate electric field on a metal-insulator-semiconductor field-effect transistor (FET) has attracted considerable interest since it is expected to be an effective tool in materials science. The active layer of the FET is formed at the interface of the semiconductor and insulator due to the increase in the local carrier concentration induced by the gate electric field. In conventional semiconductors, the channel conductivity between the source and drain increases because of the gate electric field; this phenomenon has been employed in electrical switching devices. Since the effect of the gate electric field is insufficient for a large modulation of the carrier density and is effective only in the active layer of the FET, the modulation of the macroscopic properties of materials is impossible. However, the effects of the gate electric field have been observed in Si devices,<sup>1</sup> undoped cuprates,<sup>2</sup>  $\text{VO}_2$ ,<sup>3</sup> and ferromagnetic thin films.<sup>4</sup> To study the effect of gate electric field, semiconducting materials at around their electronic phase boundary need to be investigated. In particular, there are many bis(ethylenedithio)tetrathiafulvalene (BEDT-TTF)-related complexes that commonly have a two-dimensional BEDT-TTF sheet structure. This group of materials exhibits various electronic phases as the temperature, pressure, and magnetic field are varied.<sup>5-10</sup>

BEDT-TTF and 7,7,8,8-tetracyanoquinodimethane (TCNQ) form both segregated (triclinic phase) and mixed (monoclinic phase) stacking crystals of the (BEDT-TTF)(TCNQ) charge transfer complex, which are known to be semiconductors at room temperature.<sup>11,12</sup> In particular, the triclinic phase of (BEDT-TTF)(TCNQ) undergoes a metal-insulator phase transition at 330 K.<sup>12,13</sup> The electrical resistivity of the triclinic crystal along the  $c$  axis shows a minimum at 330 K and ambient pressure. Further, it is known that the metal-insulator transition temperature ( $T_{MI}$ ) decreases with increasing hydrostatic pressures,<sup>13</sup> which is due to the modulation of the intermolecular transfer integral and band filling.<sup>14,15</sup> In addition, anisotropic thermoelectric power experiments have revealed that holes are the main carrier below  $T_{MI}$ , while electrons are dominant in the total conductivity above  $T_{MI}$ .<sup>12</sup> However, no anomaly is seen at around  $T_{MI}$  in the electron spin resonance,<sup>13</sup>  $^{13}\text{C}$ -NMR, and  $^1\text{H}$ -NMR measurements.<sup>16</sup> Furthermore, the BEDT-TTF layer is a two-dimensional Mott-Hubbard system; this was

revealed in a  $^{13}\text{C}$ -NMR experiment.<sup>16</sup> The localized spin on the BEDT-TTF molecule exhibits antiferromagnetic ordering below 20 K. In addition, one-dimensional TCNQ columns also exhibit antiferromagnetic ordering below 3 K.<sup>13</sup> Then, both BEDT-TTF layer and TCNQ columns act as Mott insulators.

In this paper, we present ambipolar FET characteristics and the temperature dependence of the source current using (BEDT-TTF)(TCNQ) crystals grown by a cast method. The crystal orientation of the grown crystals is characterized by x-ray diffraction. We observed the temperature variation in the  $I_S$ - $V_{DS}$  curves at various applied gate voltages.

## II. EXPERIMENTAL DETAILS

Source materials of BEDT-TTF and TCNQ powder with 98% purity were purchased from Tokyo Chemical Industry Co., Ltd. A highly doped  $n$ -type Si substrate with thermally oxidized  $\text{SiO}_2$  with a thickness of approximately 300 nm was used as the substrate. Au/Cr source and drain electrodes were formed on the  $\text{SiO}_2$  substrate using standard vacuum evaporation and photolithographic techniques. The gap between these parallel electrodes was approximately 13  $\mu\text{m}$ . A chloroform solution of (BEDT-TTF)(TCNQ) ( $1.0 \times 10^{-4}$  mol/ $\ell$ ) was prepared by mixing the TCNQ and BEDT-TTF solutions. The solution was dropped on the substrate surface and dried in a nitrogen atmosphere at room temperature. It has been reported that triclinic crystals were predominantly obtained by means of a solution process.<sup>12</sup> Many needlelike crystals of (BEDT-TTF)(TCNQ) with periodic and parallel ordering of the crystal arrangement grew on the surface of the  $\text{SiO}_2/\text{Si}$  substrate. The typical dimensions of the grown crystal were  $0.4 \times 300 \times 0.1 \mu\text{m}^3$ . The long axis of the needlelike crystals directly bridged the source and drain electrodes.

## III. RESULTS AND DISCUSSION

The x-ray diffraction patterns of the (BEDT-TTF)(TCNQ) powder and crystals grown on the  $\text{SiO}_2/\text{Si}$  surface are shown in Fig. 1. The diffraction peaks of the (100), (200), (300), (010), (001), and (400) planes were observed in the diffraction pattern of the powder sample. The observation of the high-order ( $h00$ ) diffraction peaks suggests high crystallinity.

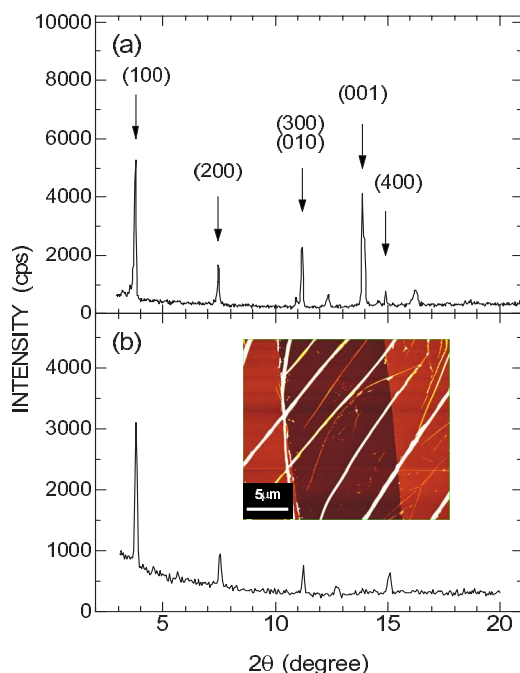


FIG. 1. (Color online) X-ray diffraction patterns of (a) (BEDT-TTF)(TCNQ) powder and (b) crystals grown on the  $\text{SiO}_2/\text{Si}$  surface. Inset: atomic force microscope image of the crystals grown around the source and drain electrodes.

The crystal structure of the triclinic phase has been reported to consist of two-dimensional BEDT-TTF sheets parallel to the (100) planes and one-dimensional TCNQ columns along the  $c$  axis.<sup>12</sup> However, in the diffraction patterns of the crystals grown on the  $\text{SiO}_2$  surface [Fig. 1(b)], the (001) and (010) diffraction peaks were not observed; this indicates that the (100) plane of the crystals is parallel to the substrate surface. In addition, the needlelike crystals whose long axis corresponds to the  $c$  axis of the crystal structure bridge the source and drain electrodes, as shown in the inset of Fig. 1(b). Therefore, the BEDT-TTF and TCNQ layers of the triclinic crystals are parallel to the substrate surface and are continuous between the source and drain electrodes.<sup>12</sup> For this orientation, the density of the BEDT-TTF or TCNQ molecule in the (100) plane at the interface of the gate insulator is  $3.98 \times 10^{18} \text{ m}^{-2}$ , which is estimated from the lattice parameters of (BEDT-TTF)(TCNQ).<sup>12</sup> Although few monoclinic crystals may coexist, their contribution to the electrical conductance will be low, because the resistivity of the monoclinic phase is  $10^7$  times higher than that of the triclinic phase.

Figure 2 shows the ambipolar FET characteristics of (BEDT-TTF)(TCNQ) crystals measured at room temperature. FET characteristics in Fig. 2(a) show the  $n$ -channel accumulation-mode operation when the drain voltage ( $V_{\text{DS}}$ ) is lower than the gate voltage ( $V_{\text{GS}}$ ). The main carrier for this operation is the electrons injected from the source electrode. The source current ( $I_{\text{S}}$ ) gets saturated when  $V_{\text{DS}}$  is equal to or slightly greater than  $V_{\text{GS}}$ . When  $V_{\text{DS}}$  is greater than  $V_{\text{GS}}$ ,  $I_{\text{S}}$  abruptly increases, indicating that the injection of holes into the (BEDT-TTF)(TCNQ) crystal from the drain electrode becomes effective. Thus, both electrons and holes are

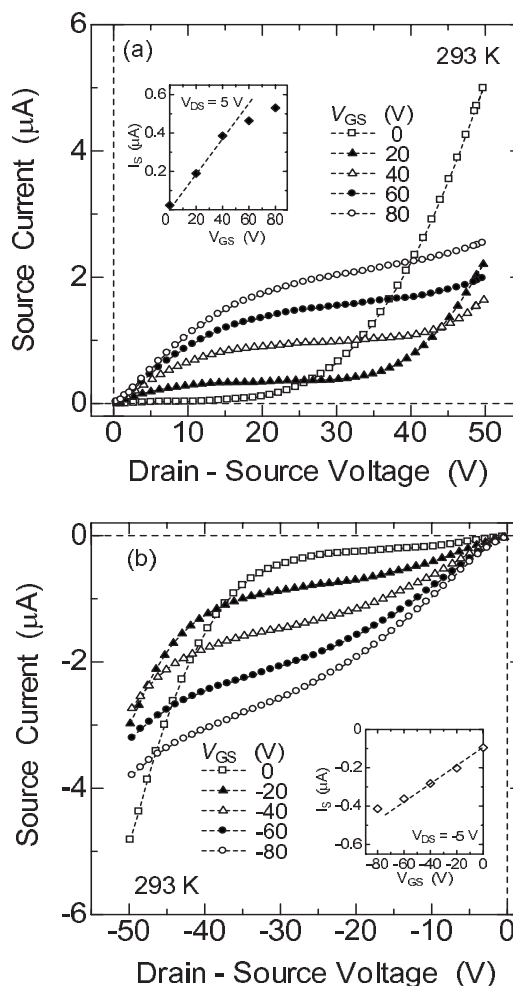


FIG. 2. Ambipolar FET characteristics of (BEDT-TTF)(TCNQ) crystals at room temperature. Inset: Transfer characteristics at  $V_{\text{DS}} = 5$  and  $-5$  V, respectively.

simultaneously injected into the (BEDT-TTF)(TCNQ) crystals from the Au electrodes. The ambipolar FET characteristics with a negative  $V_{\text{GS}}$  value also appear in the negative  $V_{\text{DS}}$  region as shown in Fig. 2(b). Transfer characteristics shown in the inset of Fig. 2 indicate that hole is dominant carrier at  $V_{\text{GS}} = 0$  V and the electron mobility is greater than the hole mobility. Although a precise estimation of the carrier mobility is difficult because the effective channel width and length of all the crystals are indeterminable, the estimated electron and hole mobilities are  $(0.6-3) \times 10^{-2}$  and  $(0.4-2) \times 10^{-2} \text{ cm}^2/\text{V s}$ , respectively.

Ambipolar carrier conduction in organic FETs has been observed in carrier-injection improved FETs,<sup>17-26</sup> double-layered thin films of  $p$ - and  $n$ -type organic semiconductors,<sup>27-38</sup> and Mott insulators.<sup>39</sup> For the double-layered thin films,<sup>27-38</sup> the conduction paths of the electrons and holes are separated into acceptor and donor layers, respectively, because the interaction between the acceptor and donor layers is very weak. On the other hand, for Mott insulators,<sup>39</sup> both the donor and acceptor bands are half filled because of dimerization and charge transfer from the donor to the acceptor; as a result, carrier transport is dominated by Coulomb interactions. However, in the case of the FET using

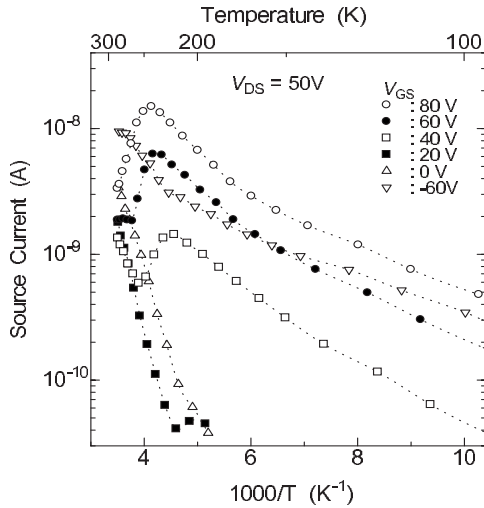


FIG. 3. Temperature dependence of  $I_S$  for various gate voltages and a drain voltage of 50 V. The dashed lines are included as a guide to the eyes.

Mott insulators, Newns *et al.* demonstrated that the excess carriers injected into the Mott insulator are undisturbed by Coulomb repulsion.<sup>2</sup> Furthermore, according to the theoretical calculation,<sup>40</sup> ambipolar carrier injection is incidental in a Mott insulator even if the Fermi energy of the crystal is quite different from that of the electrodes. In substance, ambipolar FET characteristics were also observed in the (BEDT-TTF)(TCNQ) crystalline FET when we used Al as the source and drain electrodes.

The temperature dependence of the source current at a drain voltage of 50 V and various gate voltages of  $-60$ ,  $0$ ,  $20$ ,  $40$ ,  $60$ , and  $80$  V is shown in Fig. 3. The source current decreased with decreasing temperature at a gate voltage of  $0$  V, exhibiting semiconducting behavior; the estimated activation energy was  $0.25$  eV. Although it is not shown in Fig. 3, the thermal activation energy of  $0.070$  eV is also estimated below  $210$  K. These values correspond to a previous observation of bulk (BEDT-TTF)(TCNQ).<sup>12</sup> The temperature dependence of  $I_S$  at a gate voltage of  $20$  V also exhibited thermal activation behavior for an activation energy of  $0.25$  eV. On the other hand, the source currents for gate voltages of  $60$  and  $40$  V decreased as the temperature decreased at around room temperature. Nevertheless, these source currents began to increase below  $270$  and  $260$  K, exhibiting a maximum at  $240$  and  $220$  K, respectively. The  $I_S$  value for an applied gate voltage of  $80$  V increased with decreasing temperature; it then decreased with decreasing temperature below  $240$  K. The estimated thermal activation energies for a gate voltage of  $80$  V are approximately  $0.14$  eV from  $230$  to  $170$  K and  $0.035$  eV below  $170$  K. While the source current decreases with decreasing temperature at a negative gate voltage of  $-60$  V, two different activation energies exist:  $0.17$  eV from  $280$  to  $220$  K and  $0.030$  eV below  $220$  K.

When a drain voltage of  $50$  V and gate voltages of  $0$  or  $20$  V were applied, bulk conduction dominated the total electrical conductance of the FET because the local conductance of the channel region ( $G_{\text{channel}}$ ), which is limited by the gate-drain voltage ( $V_{\text{GD}}$ ), was lower than the bulk conductance

( $G_{\text{bulk}}$ ). When gate voltages of  $40$  and  $60$  V were applied,  $G_{\text{bulk}}$  becomes greater than  $G_{\text{channel}}$  at around the room temperature. However,  $G_{\text{channel}}$  exceeded  $G_{\text{bulk}}$  with decreasing  $G_{\text{bulk}}$  at lower temperatures. When a gate voltage of  $80$  V was applied,  $G_{\text{channel}}$  was greater than  $G_{\text{bulk}}$  because of the high carrier concentration in the channel. Thus, the local conduction in the channel dominated the total conductance. Since a continuous electron accumulation layer from the source to drain is necessary for metal-like conduction, a metal-like behavior does not appear in the saturation region of the FET operation (see  $V_{\text{GS}}=20$  V in Fig. 3). Thus, the temperature variation in the source current with a fixed drain voltage of  $20$  V and applied gate voltages of  $20$ ,  $40$ ,  $60$ , and  $80$  V (not shown) has only a single maximum at around  $240$  K, because the continuous electron accumulation layer through the channel exists in the linear region of the FET operation ( $V_{\text{GD}} \geq 0$ ). In addition, the observed metal-like conduction exhibits a certain amount of sample dependence because the  $G_{\text{channel}}/G_{\text{bulk}}$  ratio depends on the crystal thickness. If a thick crystal is used, metal-like conduction is hardly observed even for a gate voltage of  $80$  V because  $G_{\text{bulk}}$  exceeds  $G_{\text{channel}}$ , which suggests that the observed metal-like conduction is a local phenomenon in the channel region.

The thermal activation energies of  $0.070$  and  $0.25$  eV correspond to a thermal generation of two types of carriers in the bulk because they vanish under a fixed carrier concentration due to the applied gate electric field. Since thermoelectric power measurements<sup>12</sup> have revealed that the dominant carrier in the bulk in the low-temperature region are holes, and the total conductivity is dominated by electrons above  $T_{\text{MI}}$ , the thermal activation energy of  $0.070$  eV corresponds to the temperature dependence of the hole concentration ( $p_{\text{thermal}}$ ). Further, we tentatively assign that the thermal activation energy of  $0.25$  eV mainly corresponds to the temperature dependence of electron concentration ( $n_{\text{thermal}}$ ). On the other hand, thermal activation energies under positive and negative gate operations depend on the applied gate voltages. Since the carrier density in the channel region is fixed by the gate electric field and exceeds that of the bulk, the thermal activation energies arise from the temperature dependence of the carrier mobility or carrier injection. To discuss the origin of these activation energies, we investigate the temperature variation in the  $I_S$ - $V_{\text{DS}}$  curves for a fixed gate voltage.

Figure 4 shows the temperature variation in the  $I_S$ - $V_{\text{DS}}$  curves at an applied gate voltage of  $80$  V. The  $I_S$  value increases with decreasing temperature from  $280$  to  $236$  K. These  $I_S$ - $V_{\text{DS}}$  curves are proportional to the  $V_{\text{DS}}$  value at around zero  $V_{\text{DS}}$ , indicating an Ohmic junction in the  $n$ -channel operation of the FET. However, the curvature of the  $I_S$ - $V_{\text{DS}}$  curve at around zero  $V_{\text{DS}}$  becomes a non-Ohmic junction below  $236$  K, which indicates the formation of an energy gap or abrupt change in the carrier conduction to thermal-activation-type mobility; both of them would arise if a structural phase transition occurred. In substance, the corresponding thermal activation behavior with an activation energy of  $0.14$  eV was observed between  $170$  and  $230$  K in Fig. 3. In addition, the curvature of the  $I_S$ - $V_{\text{DS}}$  curves at around zero  $V_{\text{DS}}$  at an applied negative gate voltage of  $-60$  V

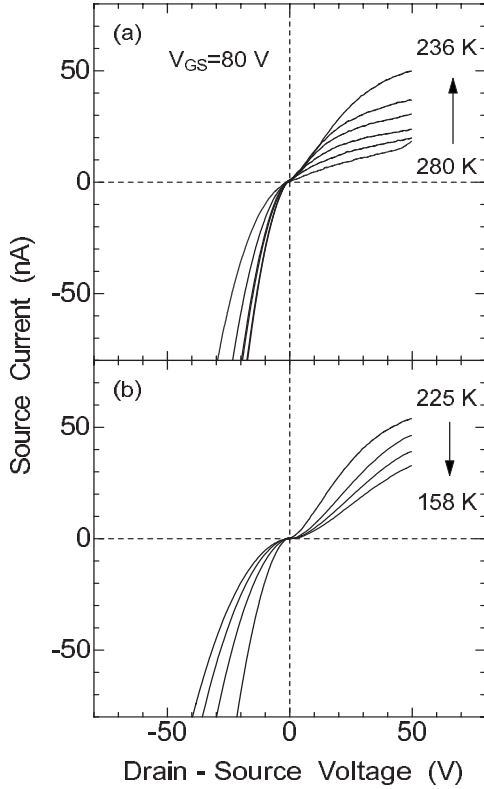


FIG. 4. Temperature variation in the  $I_S$ - $V_{DS}$  curve for an applied gate voltage of 80 V (a) from 280 to 236 K and (b) from 225 to 158 K.

(not shown) also exhibits a similar temperature variation showing a change from an Ohmic to a non-Ohmic junction at around 270 K with the corresponding activation energy of 0.17 eV. On the other hand, the  $I_S$ - $V_{DS}$  curves at an applied gate voltage of 0 V shown in Fig. 5, which indicate bulk conduction, exhibit no anomaly with respect to the curvature. Comparing these results for zero and nonzero gate voltages, it is speculated that the origin of these transitions arise from the conduction paths of the accumulated electrons and holes, and not in the bulk. However, the origin of this change is still an open question because it is difficult to perform x-ray diffraction, magnetic experiments, and other measurements to detect the channel region of the FET.

On the other hand, in the metal-like region above 240 K under a gate voltage of 80 V, electrons are the dominant carrier in the linear region of the positive gate operation. The bulk conductivity ( $\sigma_{\text{bulk}}^e$ ) and channel conductivity ( $\sigma_{\text{channel}}^e$ ) in this region are

$$\sigma_{\text{bulk}}^e = en_{\text{thermal}}\mu_{\text{bulk}}^e,$$

$$\sigma_{\text{channel}}^e = en_{\text{induced}}\mu_{\text{channel}}^e,$$

where  $\mu_{\text{bulk}}^e$  and  $\mu_{\text{channel}}^e$  are the electron mobilities in the bulk and channel regions, respectively.  $n_{\text{thermal}}\mu_{\text{bulk}}^e$  decreases with decreasing temperature at an activation energy of 0.25 eV. On the other hand,  $n_{\text{induced}}$  is the local density of electrons induced by the gate electric field in the channel

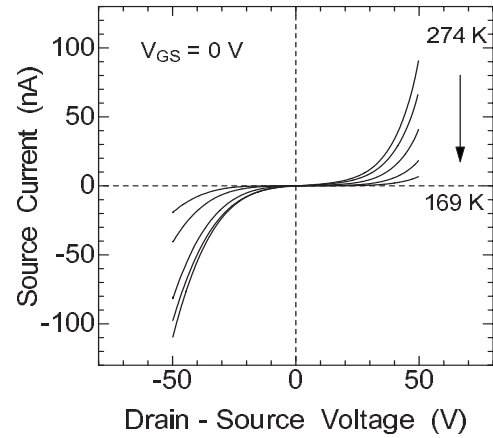


FIG. 5. Temperature variation in the  $I_S$ - $V_{DS}$  curve for an applied gate voltage of 0 V from 274 to 169 K.

region; it is independent of temperature and fixed by the distribution of the electric field in the channel region. Therefore, we propose that the metal-like behavior observed above 240 K is due to the temperature dependence of  $\mu_{\text{channel}}^e$ .

One possible explanation for this phenomenon is the gate-induced shift in  $T_{\text{MI}}$ . By using a simple capacitor model, the density of electrons at a gate voltage of 80 V was estimated to be  $5.6 \times 10^{16} \text{ m}^{-2}$ ; this corresponds to 0.014 electrons/molecule in the (100) plane determined using the estimated density of molecules. This excess electron density will be generally insufficient for the gate-induced Mott transitions due to the modulation of band filling. However, the lower shift in  $T_{\text{MI}}$  may be promoted by the small number of induced carriers. For example, the  $T_{\text{MI}}$  value of bulk (BEDT-TTF)(TCNQ) is reduced by the application of hydrostatic pressures.<sup>13</sup> In this case, a large reduction in  $T_{\text{MI}}$  can be attributed to the changes in both intermolecular transfer and band filling. Another possible explanation for the metal-like temperature dependence is that the genuine  $T_{\text{MI}}$  value of (BEDT-TTF)(TCNQ) bulk is 240 K. In substance, one can observe an anomaly at around 240 K in the anisotropic thermoelectric power.<sup>12</sup> According to this assumption, the discrepancy between  $T_{\text{MI}}$  defined by  $\sigma$  (330 K) and  $\mu_{\text{channel}}^e$  (240 K) can be explained by the large difference in the temperature dependence of  $n_{\text{thermal}}$  and  $\mu_{\text{channel}}^e$ .

In summary, the ambipolar carrier conduction induced by a gate electric field is observed in (BEDT-TTF)(TCNQ) crystals. The temperature dependence of  $I_S$  exhibited a metal-like behavior in the electron accumulation mode above 240 K. The temperature dependence of  $I_S$  transforms into thermal-activation-type behavior below 240 K with a corresponding change in the curvature of the  $I_S$ - $V_{DS}$  curve. Although the origin of this change has still not been investigated, it has been proposed that this phenomenon occurs in the channel region of the FET.

#### ACKNOWLEDGMENT

The authors are grateful to T. Mori for fruitful discussions.

- \*Corresponding author. sakai@faculty.chiba-u.jp
- <sup>1</sup>E. Abrahams, S. V. Kravchenko, and M. P. Sarachik, *Rev. Mod. Phys.* **73**, 251 (2001).
  - <sup>2</sup>D. M. Newns, J. A. Misewich, C. C. Tsuei, A. Gupta, B. A. Scott, and A. Schrott, *Appl. Phys. Lett.* **73**, 780 (1998).
  - <sup>3</sup>H. T. Kim, B. G. Chae, D. H. Youn, S. L. Maeng, G. Kim, K. Y. Kang, and Y. S. Lim, *New J. Phys.* **6**, 52 (2004).
  - <sup>4</sup>H. Ohno, D. Chiba, F. Matsukura, T. Omiya, E. Abe, T. Dietl, Y. Ohno, and K. Ohtani, *Nature (London)* **408**, 944 (2000).
  - <sup>5</sup>H. Ito, T. Ishiguro, M. Kubota, and G. Saito, *J. Phys. Soc. Jpn.* **65**, 2987 (1996).
  - <sup>6</sup>T. Ishiguro, H. Ito, Y. Yamauchi, E. Ohmichi, M. Kubota, H. Yamochi, G. Saito, M. V. Kartsovnik, M. A. Tanatar, Y. V. Suskhko, and G. Y. Logvenov, *Synth. Met.* **85**, 1471 (1997).
  - <sup>7</sup>H. Taniguchi, A. Kawamoto, and K. Kanoda, *Physica C* **388**, 597 (2003).
  - <sup>8</sup>P. Limelette, P. Wzietek, S. Florens, A. Georges, T. A. Costi, C. Pasquier, D. Jerome, C. Meziere, and P. Batail, *Phys. Rev. Lett.* **91**, 016401 (2003).
  - <sup>9</sup>F. Kagawa, T. Itou, K. Miyagawa, and K. Kanoda, *Phys. Rev. Lett.* **93**, 127001 (2004).
  - <sup>10</sup>F. Kagawa, T. Itou, K. Miyagawa, and K. Kanoda, *Phys. Rev. B* **69**, 064511 (2004).
  - <sup>11</sup>T. Mori and H. Inokuchi, *Bull. Chem. Soc. Jpn.* **60**, 402 (1987).
  - <sup>12</sup>T. Mori and H. Inokuchi, *Solid State Commun.* **59**, 355 (1986).
  - <sup>13</sup>Y. Iwasa, K. Mizuhashi, T. Koda, Y. Tokura, and G. Saito, *Phys. Rev. B* **49**, 3580 (1994).
  - <sup>14</sup>R. H. Friend, M. Miljak, and D. Jerome, *Phys. Rev. Lett.* **40**, 1048 (1978).
  - <sup>15</sup>A. Andrieux, H. J. Schulz, D. Jerome, and K. Bechgaard, *Phys. Rev. Lett.* **43**, 227 (1979).
  - <sup>16</sup>A. Kawamoto, K. Miyagawa, A. Shimizu, and K. Kanoda, *Synth. Met.* **85**, 1601 (1997).
  - <sup>17</sup>S. Kobayashi, T. Nishikawa, T. Takenobu, S. Mori, T. Shimoda, T. Mitani, H. Shimotani, N. Yoshimoto, S. Ogawa, and Y. Iwasa, *Nat. Mater.* **3**, 317 (2004).
  - <sup>18</sup>T. Yasuda, T. Goto, K. Fujita, and T. Tsutsui, *Appl. Phys. Lett.* **85**, 2098 (2004).
  - <sup>19</sup>J. Reynaert, D. Cheyns, D. Janssen, R. Müller, V. I. Arkhipov, J. Genoe, G. Borghs, and P. Heremans, *J. Appl. Phys.* **97**, 114501 (2005).
  - <sup>20</sup>R. J. Chesterfield, C. R. Newman, T. M. Pappenfus, P. C. Ewbank, M. H. Haukaas, K. R. Mann, L. L. Miller, and C. D. Frisbie, *Adv. Mater. (Weinheim, Ger.)* **15**, 1278 (2003).
  - <sup>21</sup>T. Nishikawa, S. Kobayashi, T. Nakanowatari, T. Mitani, T. Shimoda, Y. Kubozono, G. Yamamoto, H. Ishii, M. Niwano, and Y. Iwasa, *J. Appl. Phys.* **97**, 104509 (2005).
  - <sup>22</sup>T. B. Singh, F. Meghdadi, S. Günes, N. Marjanovic, G. Horowitz, P. Lang, S. Bauer, and N. S. Sariciftci, *Adv. Mater. (Weinheim, Ger.)* **17**, 2315 (2005).
  - <sup>23</sup>T. Takahashi, T. Takenobu, J. Takeya, and Y. Iwasa, *Appl. Phys. Lett.* **88**, 033505 (2006).
  - <sup>24</sup>Y. Takahashi, T. Hasegawa, Y. Abe, Y. Tokura, and G. Saito, *Appl. Phys. Lett.* **88**, 073504 (2006).
  - <sup>25</sup>T. Yasuda and T. Tsutsui, *Jpn. J. Appl. Phys., Part 2* **45**, L595 (2006).
  - <sup>26</sup>T. B. Singh, P. Senkarabacak, N. S. Sariciftci, A. Tanda, C. Lackner, R. Hagelauer, and G. Horowitz, *Appl. Phys. Lett.* **89**, 033512 (2006).
  - <sup>27</sup>A. Dodabalapur, H. E. Katz, L. Torsi, and R. C. Haddon, *Appl. Phys. Lett.* **68**, 1108 (2004).
  - <sup>28</sup>Y. Sakamoto, T. Suzuki, M. Kobayashi, Y. Gao, Y. Fukai, Y. Inoue, F. Sato, and S. Tokito, *J. Am. Chem. Soc.* **126**, 8138 (2004).
  - <sup>29</sup>C. Rost, D. J. Gundlach, S. Karg, and W. Riess, *Appl. Phys. Lett.* **85**, 1613 (2004).
  - <sup>30</sup>E. Kuwahara, Y. Kubozono, T. Hosokawa, T. Nagano, and K. Masunari, *Appl. Phys. Lett.* **85**, 4765 (2004).
  - <sup>31</sup>C. Rost, D. J. Gundlach, S. Karg, and W. Riess, *J. Appl. Phys.* **95**, 5782 (2004).
  - <sup>32</sup>J. Wang, H. Wang, X. Yan, H. Huang, and D. Yan, *Appl. Phys. Lett.* **87**, 093507 (2005).
  - <sup>33</sup>R. Ye, M. Baba, Y. Oishi, K. Mori, and K. Suzuki, *Appl. Phys. Lett.* **86**, 253505 (2005).
  - <sup>34</sup>G. Paasch, T. Lindner, C. Rost-Bietsch, S. Karg, W. Riess, and S. Scheinert, *J. Appl. Phys.* **98**, 084505 (2005).
  - <sup>35</sup>M. A. Loi, C. Rost-Bietsch, M. Murgia, S. Karg, W. Riess, and M. Muccini, *Adv. Funct. Mater.* **16**, 41 (2006).
  - <sup>36</sup>J. Wang, H. Wang, X. Yan, H. Huang, D. Jin, J. Shi, Y. Tang, and D. Yan, *Adv. Funct. Mater.* **16**, 824 (2006).
  - <sup>37</sup>H. Wang, J. Wang, X. Yan, J. Shi, H. Tian, Y. Geng, and D. Yan, *Appl. Phys. Lett.* **88**, 133508 (2006).
  - <sup>38</sup>F. Dinelli, R. Capelli, M. A. Loi, M. Murgia, M. Muccini, A. Facchetti, and T. J. Marks, *Adv. Mater. (Weinheim, Ger.)* **18**, 1416 (2006).
  - <sup>39</sup>T. Hasegawa, K. Mattenberger, J. Takeya, and B. Batlogg, *Phys. Rev. B* **69**, 245115 (2004).
  - <sup>40</sup>K. Yonemitsu, *J. Phys. Soc. Jpn.* **74**, 2544 (2005).